Mechanism of Hydrolysis of Primary and Secondary Enamines[1]

James K. Coward[2] and Thomas C. Bruice[3]

Contribution from the Department of Chemistry,
University of California at Santa Barbara, Santa Barbara, California 93106.
Received February 10, 1969

Abstract: The kinetics of the hydrolysis of six primary and ten secondary enamines has been investigated. The rate-determining step at pH >2 is tautomerization of the enamine to the protonated ketimine, which is rapidly hydrolyzed by water. Below pH 2, a change in the rate-determining step occurs, so that hydrolysis of the protonated enamine is the slower reaction, preceded by a rapid preequilibrium tautomerization step. Large nonspecific inhibitory solvent effects are observed in the pH region where the tautomeric change is rate determining. Substituent effects at various positions in the enamine molecules, coupled with the general-acid catalysis observed (β = 0.65), suggest a transition state with considerable bond making in the protonation of the enamine carbon–carbon double bond. These mechanistic conclusions are discussed in relation to enzyme-catalyzed aldol condensations and decarboxylations, in which ketimine–enamine tautomerization is involved.

Schiff base intermediates have been demonstrated in several enzymatic reactions.[4] It is generally accepted that conversion of the Schiff base to an enamine precedes the aldol condensation in the case of the aldolases,[4a] and accompanies decarboxylation in the case of decarboxylases.[4b] Recently, the existence of an enamine intermediate in the enzymatic decarboxylation of acetoacetic acid has been clearly demonstrated by exchange experiments.[5] Indeed, irreversible inhibition of acetoacetate decarboxylase can be accomplished by use of ketones capable of forming stable enamines, *e.g.*, acetopyruvic acid[6a] and acetylacetone.[6b]

These data support a similar mechanistic pathway for enzyme-catalyzed aldol-type condensation and decarboxylation as depicted in the following series of reactions (see Scheme I). That such a similar sequence of reactions is involved in both aldolases and decarboxylases is supported by the observation that 4-hydroxy-2-ketoglutarate aldolase catalyzes the decarboxylation of acetoacetic acid.[7] It is readily apparent that a series of prototropic shifts involving interconversion of the ketimine–enamine tautomers are critical in this type of enzymatic catalysis.

The literature contains little information on the rate of this interconversion in nonenzymatic systems. In a series of papers, Hine and coworkers[8] have studied dedeuteration of protonated imines of isobutyraldehyde-2-*d*, the aldimine analog of reaction b, Scheme I. Bender and Williams[9] have studied the amine-catalyzed enolization of acetone, a more suitable model of reaction b, Scheme I. Ignoring the many problems associated with iodination of ketones,[10] one may attempt to relate

Scheme I

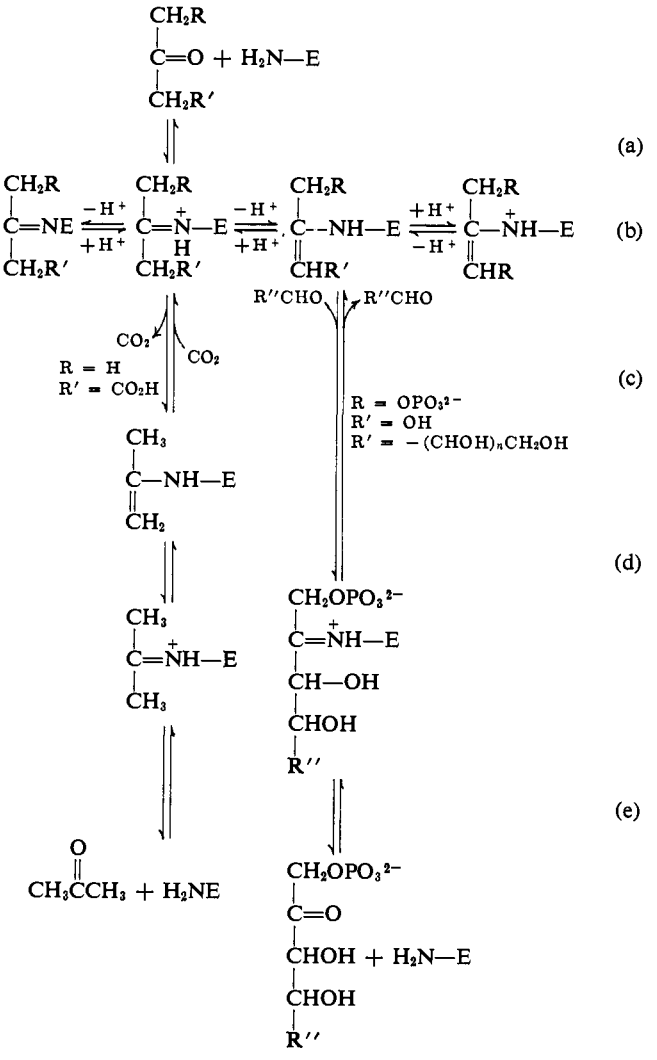

(1) Part XII in the series on Catalytic Reactions Involving Azomethines. For previous papers, see T. C. Bruice and R. M. Topping, *J. Amer. Chem. Soc.*, **85**, 1480, 1488, 1493 (1963); T. C. French and T. C. Bruice, *Biochemistry*, **3**, 1589 (1964); T. C. French, D. S. Auld, and T. C. Bruice, *ibid.*, **4**, 77 (1965); J. W. Thanassi, A. R. Butler, and T. C. Bruice, *ibid.*, **4**, 1463 (1965); D. S. Auld and T. C. Bruice, *J. Amer. Chem. Soc.*, **89**, 2083, 2090, 2098 (1967); J. R. Maley and T. C. Bruice, *ibid.*, **90**, 2843 (1968); T. C. Bruice and A. Lombardo, *ibid.*, **91**, 3009 (1969).

(2) Postdoctoral Fellow, National Institutes of Health, 1966–1968.

(3) To whom inquiries should be directed.

(4) (a) B. L. Horecker in "Comprehensive Biochemistry," Vol. 15, M. Florkin and E. H. Stotz, Ed., Elsevier Publishing Co., New York, N. Y., 1964, p 48. (b) F. H. Westheimer, *Proc. Chem. Soc.*, 253 (1963). (c) T. C. Bruice and S. J. Benkovic, "Bioorganic Mechanisms," Vol. II, W. A. Benjamin, Inc., New York, N. Y., 1966, Chapter 8; (d) D. Portsmouth, A. C. Stoolmiller, and R. H. Abeles, *J. Biol. Chem.*, **242**, 2751 (1967).

(5) W. Tagaki and F. H. Westheimer, *Biochemistry*, 7, 901 (1968).

(6) (a) W. Tagaki, J. P. Guthrie, and F. H. Westheimer, *ibid.*, 7, 905 (1968); (b) I. Fridovich, *J. Biol. Chem.*, **243**, 1043 (1968).

(7) R. D. Kobes and E. E. Dekker, *Biochem. Biophys. Res. Commun.*, 27, 607 (1967).

(8) J. Hine, F. E. Rogers, and R. E. Notari, *J. Amer. Chem. Soc.*, **90**, 3279 (1968), and previous papers in this series.

(9) M. L. Bender and A. Williams, *ibid.*, **88**, 2502 (1966).

(10) For a discussion of these problems and limitations of this technique of monitoring keto–enol tautomerization, see the accompanying

quantitatively the reported data[9] to Scheme Ib. However, in order to accomplish this, the dissociation constant of the protonated imine must be known. Unfortunately these data are not available for either the protonated aldimine[8] or ketimine.[9]

Stabilization of the enamine form of ketimines derived from β-keto nitriles, β-keto esters, and β-diketones is well documented in the literature.[11] Formation of dihydropyridines by reaction of ketones and aldehydes with enamines of this type[12] presumably involves an initial attack by the carbonyl group, analogous to the aldolase reaction. The reaction of such enamines with a proton should serve as a nonenzymatic model for reactions involving electrophilic attack on enamines in biological systems. Acid-catalyzed hydrolysis of these enamines to the corresponding ketone has been appreciated for many years.[13]

Hydrolysis of tertiary enamines has been investigated by Stamhuis, *et al.*[14] However, many facets of this work appear to be ambiguous (see Discussion). In addition, the proposed enzymatic reaction intermediates are secondary enamines, and thus more suitable models for the enzymatic catalysis would appear to be those involving ketimine–secondary enamine tautomerism. A kinetic investigation of the hydrolysis of several enamines (Chart I) of a type similar to the proposed en-

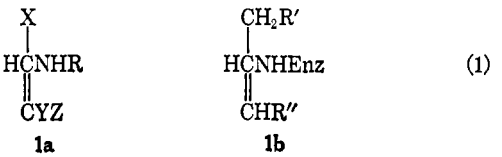

(1)

1a **1b**

zyme–enamine intermediate, *i.e.*, **1a** *vs.* **1b**, was carried

Chart I. Structure of Enamines

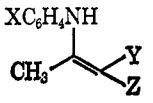

1a, X = H; Y = CN; Z = H
b, X = CH_3; Y = CN; Z = H
c, X = $N(CH_3)_2$; Y = CN; Z = H
d, X = COOH; Y = CN; Z = H
e, X = Cl; Y = CN; Z = H
f, X = OCH_3; Y = CN; Z = H
g, X = H; Y = CO_2Et; Z = H
h, X = H; Y = CO_2Et; Z = CN
i, X = H; Y = CN; Z = CN

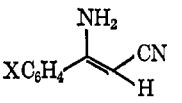

2a, X = H
b, X = CH_3
c, X = $N(CH_3)_2$
d, X = COOH
e, X = Cl
f, X = OCH_3

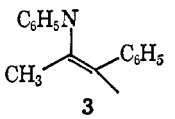

3

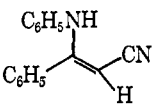

4

out in an attempt to elucidate details of the mechanism of this type of prototropy, and related enzyme-catalyzed processes.

paper: J. K. Coward and T. C. Bruice, *J. Amer. Chem. Soc.*, 91, 5339 (1969).

(11) (a) R. W. Layer, *Chem. Rev.*, 63, 489 (1963); (b) S. Baldwin, *J. Org. Chem.*, 26, 489 (1961); (c) F. C. Pennington and W. D. Kahret, *ibid.*, 32, 2034 (1967).

(12) "Chemistry of Carbon Compounds," Vol. IV, E. H. Rodd, Ed., Elsevier Publishing Co., New York, N. Y., 1957, p 498.

(13) See, for example, E. von Meyer, *J. Prakt. Chem.*, [2] 78, 501 (1908).

(14) (a) E. J. Stamhuis and W. Maas, *J. Org. Chem.*, 30, 2156 (1965); (b) W. Mass, M. J. Janssen, E. J. Stamhuis, and H. Wynberg, *ibid.*, 32, 1111 (1967).

Experimental Section

Materials. Ethyl β-anilinocrotonate (Eastman Kodak) was distilled, and β-aminocinnamonitrile (Aldrich) was recrystallized from ethanol–water. The physical properties of these and all other enamines used in this study are listed in Table I. The synthetic methods employed to prepare the various enamines are listed in Table I and described below. No attempt was made to maximize yields.

Table I. Synthetic Procedures, Physical Properties, and Analyses of Enamines[a]

Enamine	Procedure	Bp (mm) or mp, °C	Lit. bp (mm) or mp, °C	λ_{max}, mμ
1a	A	117–119	116–117[b]	283
1b	A	98–103	102[c]	286
1c	A	156.5–158	151[d]	286
1d				
1e	A	113–115	114[e]	290
1f	A	123–125	123[d]	280
1g		137–138 (3.5)	128–130 (2.0)[e]	296
1h	B	84–85[f]		292
1i	C	192–194	193–194[g]	286
2a		84.5–87.5	86[h]	286
2b	D	107–110	108[i]	290
2c	D	214–216	210[j]	310[k]
2d	E	257–262 dec[l]		295
2e	D	140–144	144[m]	294
2f	D	117–118	118[n]	245[k]
3	F	118–123 (1)[o]		280
4	G	126–137[p]	125–136[q]	310[r]

[a] All analyses were performed by A. Bernhardt, Max-Planck Institute, Mülheim, Germany. [b] H. Adkins and G. M. Whitman, *J. Amer. Chem. Soc.*, 64, 150 (1942). [c] See ref 13. [d] E. von Meyer, *J. Prakt. Chem.*, [2] 92, 192 (1915). [e] $n^{23}D$ 1.5778 (lit. $n^{25}D$ 1.5770). G. A. Reynolds and C. R. Hauser, "Organic Synthesis," Coll. Vol. III, John Wiley & Sons, Inc., New York, N. Y., 1955, p 374. [f] *Anal.* Calcd for $C_{13}H_{14}N_2O_2$: C, 67.81; H, 6.13; N, 12.17. Found: C, 67.93; H, 6.29; N, 12.04. [g] W. J. Meddleton, *J. Org. Chem.*, 31, 3731 (1966). The synthetic route employed in the cited reference is totally unlike that employed in this work. [h] Holzwart, *J. Prakt. Chem.*, [2] 39, 242 (1889). [i] E. von Meyer, *ibid.*, [2] 52, 110 (1895). [j] E. von Meyer, *ibid.*, [2] 92, 182 (1915). [k] Wavelength of maximum difference between spectra of starting material and product. [l] *Anal.* Calcd for $C_{10}H_8N_2O_2$: C, 63.83; H, 4.28; N, 14.89. Found: C, 63.96; H, 4.28; N, 14.77. [m] E. von Meyer, *J. Prakt. Chem.*, [2] 92, 182 (1915). [n] E. Benary and G. Schwoch, *Chem. Ber.*, 57, 335 (1924). [o] $n^{22.5}D$ 1.5838. This material decomposes rapidly on standing as expected for an anil of this type; see, for example, G. Bianchetti, D. Pocar, P. Dalla Croce, G. G. Gallo, and A. Vigervani, *Tetrahedron Lett.*, 1637 (1966). See Experimental Section for spectral characteristics. [p] *Anal.* Calcd for $C_{15}H_{12}N_2$: C, 81.79; H, 5.49; N, 12.72. Found: C, 81.74; H, 5.29; N, 12.72. [q] C. Mouer and I. Lagennec, *Bull. Soc. Chim. Fr.*, [3] 35, 1183 (1906). [r] 28.5% aqueous ethanol.

Potassium chloride, sodium formate, potassium acetate, monobasic potassium phosphate, dibasic potassium phosphate, potassium bicarbonate, and potassium carbonate were reagent grade (Baker) and were used without further purification. Chloroacetic acid (Matheson Coleman and Bell) was recrystallized from benzene (mp 61.5–63.0°) All enamines were stored in a vacuum desiccator over P_2O_5, and all aqueous solutions were prepared using doubly distilled water.

Procedure A. Aniline (1.40 g, 15 mmol) in 1.54 g (25 mmol) of glacial acetic acid was added rapidly to a suspension of 1.25 g (15 mmol) of 3-aminocrotononitrile (Aldrich) in 5 ml of water. The reaction mixture was stirred at ambient temperature for 30 min and cooled in an ice bath, and the product collected on a filter. Recrystallization gave 1.23 g (52 %) of a white crystalline material (**1a**), mp 117–119° (lit. mp 116–117°,[15] 115° [13]).

Procedure B. Aniline (9.31 g, 0.1 mol), 16.22 g (0.1 mol) of triethyl orthoacetate, and 11.31 g (0.1 mol) of ethyl cyanoacetate were heated at reflux temperature for 3.25 hr, as 11.83 g (85%) of

(15) See Table I, footnote *b*.

ethanol was removed continuously by distillation. The residue was diluted with 25 ml of ethanol and treated with decolorizing carbon, and the burgundy filtrate was concentrated *in vacuo*. Large cubic crystals separated from the residue on standing at ambient temperature for 3 days. Several recrystallizations from ethanol–water afforded 2.62 g (11.4%) of white crystals (**1h**), mp 84–85°.

Procedure C. Aniline (2.79 g, 30 mmol), 4.86 g (30 mmol) of triethyl orthoacetate, and 1.98 g (30 mmol) of malononitrile were heated at reflux temperature for 3.25 hr. A small amount of precipitate was observed on cooling at −5°. This was removed by filtration and the filtrate concentrated *in vacuo* to give a dark residue which solidified on cooling in an ice bath. Trituration of the solid mass with ether gave a beige crystalline material which was collected and washed with ether, yield 715 mg (13%), mp 192–194°. Recrystallization from ethanol gave white crystals (**1i**), mp 192–194° (lit.[16] mp 193–194°).

Procedure D. *p*-Tolunitrile (1.75 g, 15 mmol) in 25 ml of benzene was treated with 700 mg [30 mmol (1.175 g of 59.8% suspension in mineral oil)] of sodium hydride. To the resulting mixture, 1.20 g (30 mmol) of CH_3CN was added slowly and then the mixture was heated at reflux temperature for 16 hr. On cooling, a brown precipitate formed which was collected by filtration and added slowly to cold absolute ethanol, and the resulting solution poured onto ice. On warming to ambient temperature, the mixture was extracted with benzene, and the dried benzene extract concentrated *in vacuo* to give 800 mg (34%) of crude product. This crude material could be purified by dissolving in a small amount of ethyl acetate and allowing the solvent to evaporate, leaving behind yellow crystals. Trituration with ether gave a white crystalline material (**2b**), mp 107–110° (lit.[17] mp 108°).

Procedure E. This procedure is similar to procedure D, except dimethyl sulfoxide was substituted for benzene as the reaction solvent, and the reaction was run at ambient temperature. *p*-Cyanobenzoic acid (1.47 g, 10 mmol) was added slowly to 25 ml of dimethyl sulfoxide, containing 720 mg [30 mmol (1.205 g of 59.8% suspension in mineral oil)] of sodium hydride. Into the resulting mixture was added 1.20 g (30 mmol) of acetonitrile and the reaction was allowed to continue at ambient temperature for a total of 3.5 hr. The reaction mixture was poured slowly into ice–water, then acidified to pH 7 with glacial acetic acid, and the precipitate collected on a filter. Recrystallization from 2-methoxyethanol–water gave a beige powder (**2d**), yield 407 mg (22%); mp 257–262° dec.

Procedure F. N-Phenyl-α-methylphenethylidenimine (**3**) was prepared by reaction of 2.083 g (10 mmol) of 2,2-diethoxy-1-phenylacetone[18] ($n^{22}D$ 1.4838) with 1.21 g (13 mmol) of aniline at reflux temperature as 658 mg of ethanol (70%) was removed by distillation as formed over a period of 3 hr. The residue was distilled *in vacuo* and the fraction boiling at 77–81° (1 mm) was collected: yield 325 mg (15%); $n^{22.5}D$ 1.5838. The light yellow liquid appeared to be unstable, becoming darker in color over a period of only a few days at ambient temperature. In addition, the distillation residue contained considerable amounts of high-boiling viscous materials. Presumably, more complex condensation products are formed, as in the case with acetone anil.[19]

Procedure G. This procedure is similar to procedure A, except *n*-butyl alcohol was used as solvent at reflux temperature. Aniline (1.40 g, 15 mmol) in 1.54 g (25 mmol) of glacial acetic acid and 3 ml of butanol was added to 2.163 g (15 mmol) of β-aminocinnamonitrile in 5 ml of butanol, and the solution heated at reflux temperature for 2.75 hr. The solvent was removed *in vacuo*, and the solid residue crystallized from ethanol–water. Recrystallization from ethanol gave light yellow crystals (**4**), mp 126–137° (lit.[20] mp 125–136°).

All attempts to prepare **1** with electron-deficient anilines (*e.g.*, X = NO_2, Y = CN, Z = H) failed using procedures A or G. In addition, use of N,N-dimethylformamide at ambient temperature or diethylene glycol at reflux temperature as solvents failed to give the desired enamine. In all cases, *p*-nitroaniline was the only identifiable material recovered from the reaction mixture. More difficult to understand is the failure of electron-deficient benzonitriles to undergo the condensation with acetonitrile to yield **2** (*e.g.*, X = $-NO_2$, $-CO_2Et$). Nearly quantitative yields of the substituted benzonitrile were recovered from the reaction mixtures, using procedures D or E. During the course of this research, a report appeared[21] confirming the lack of reactivity of *p*-nitrobenzonitrile toward the anion of acetonitrile.

Spectral Characteristics. Although earlier workers[15] assigned the enamine structure to **1a** based on unpublished Raman spectra, it is crucial to this study to know for certain that all compounds investigated in this work are initially enamines, rather than the tautomeric imines. Infrared spectra of **1** all show characteristic absorption at 3200–3300 (–NH), 1580–1590 (aliphatic C=C), 1600–1620 cm^{-1} (aromatic C=C). In addition, in **1** where X = CN, Y = H, absorption occurs at 2200–2250 cm^{-1} (CN), whereas when X = Y = CN, a doublet at 2210, 2240 cm^{-1} (CN, CN) is observed. Ultraviolet absorption spectra of **1a–1f** exhibit a maximum at 280–290 mμ. Proton magnetic resonance spectra exhibited sharp singlets at δ 3.9–4.3, attributed to the vinyl proton. Similar assignments have been made in correlating spectra of some related enaminonitriles.[11b,22]

In the case of X = CO_2Et, Y = H (**1g**), or X = CO_2Et, Y = CN (**1h**), the enamine structure is indicated by adsorption at γ 3200–3250 cm^{-1} (N–H) and γ 1660 cm^{-1} (ester C=O) in the infrared, and the ultraviolet absorption maxima increased to 290–300 mμ. Enamines of cyclopentanonecarboxylic acid esters have been shown to exhibit similar spectral properties.[11c] The 1660-cm^{-1} absorption assigned to the ester carbonyl is typical of α-amino α,β-unsaturated esters.[23]

Similarly, the enamines **2** all exhibited multiplets at 3200–3500 cm^{-1} ($-NH_2$) together with singlets at 2190–2210 (CN) and 1580–1590 cm^{-1} (aliphatic C=O) in the infrared region. Ultraviolet absorption maxima in this series occurred at λ 286–322 mμ. Enamine **4** exhibited N–H absorption at 3230 cm^{-1}, and although the lower solubility of **4** precluded obtaining ultraviolet spectra in water, in 28.5% aqueous ethanol, λ_{max} 310 mμ.

In contrast, **3** showed only slight absorption at 3300 cm^{-1} (NH) and a slight shoulder at 1575 cm^{-1} (C=C), but exhibited a strong peak at 1650 cm^{-1} (C=N). The ultraviolet absorption at 280 mμ had an extinction coefficient of approximately 1000 as compared with extinction coefficients in the order of 10^4 observed for enamines **1**, **2**, and **4**. It would appear that **3** is predominantly in the form of the imine.

Kinetics. All kinetic measurements were done at 30 ± 0.1° in aqueous solutions at μ = 1.0 with KCl, except 28.5% aqueous ethanol was used in runs with **4**. Buffers employed were hydrochloric acid (pH 0–1.36), phosphoric acid (pH 1.85–2.25), chloroacetic acid (pH 1.80–3.62), sodium formate (pH 3.24–3.67), potassium acetate (pH 4.06–5.14), potassium hydrogen phosphate (pH 5.40–7.11), potassium bicarbonate (pH 9.19–10.14). Buffer dilutions were carried out over a range of 0.1–1.0 *M* at constant μ. The pH of the reaction solution was determined before and after each run, and all runs exhibiting pH drifts of greater than 0.03 pH unit were discarded.

The disappearance of the enamine with time was followed spectrophotometrically by recording the decrease in optical density at λ_{max} of the particular enamine (Table I). In a typical run, one drop from a disposable pipet of a 10^{-2} *M* solution of the enamine in either dioxane or acetonitrile was added to a 3-ml cuvette containing a solution of the buffer previously equilibrated at 30 ± 0.1°. The cuvette was inverted several times and immediately returned to the thermostated cell housing of the spectrophotometer for recording of the change of absorbance. The concentration of the enamine in the cuvette was *ca.* 10^{-4} *M*, and in all kinetic experiments the concentration of the buffer was at least 0.03 *M*, so that pseudo-first-order kinetics were obtained in all cases. First-order plots were linear for a minimum of two half-lives, and in most cases for more than three half-lives.

The rate constants for reactions whose half-lives were less than 2.5 sec were determined from reactions carried out on the stopped-flow spectrophotometer. In these experiments, a 1 *M* KCl solution containing *ca.* 10^{-4} *M* enamine and 1% dioxane or acetonitrile at pH *ca.* 12 with KOH was mixed with an equal volume of hydrochloric acid of known normality, previously adjusted to μ = 1.0 (with KCl). The pH was determined from a 1:1 mixture of these solutions.

The values of the pseudo-first-order rate constants (k_{obsd}) were calculated from plots of ln $[(OD_\infty - OD_0)/(OD_\infty - OD_t)]$ *vs.* time (*t*). All actual computations were carried out with an Olivetti–

(16) See Table I, footnote *g*.
(17) See Table I, footnote *i*.
(18) D. Shiho, *J. Chem. Soc. Jap.*, **65**, 237 (1945).
(19) See Table I, footnote *o*.
(20) See Table I, footnote *q*.
(21) J. Kuthan, V. Jehlicka, and E. Hakr, *Collect. Czech. Chem. Commun.*, **32**, 4309 (1967).
(22) P. M. Greaves and S. R. Landor, *Chem. Commun.*, 322 (1966).
(23) H. Fritz, E. Besch, and T. Wieland, *Ann.*, **617**, 177 (1958).

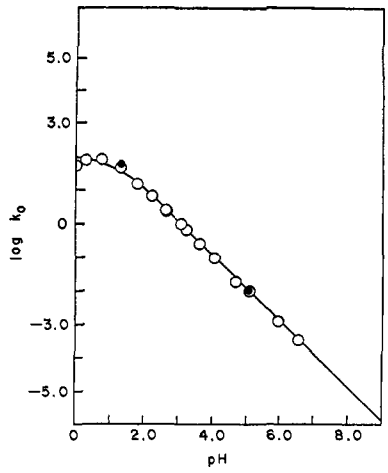

Figure 1. Spectrophotometrically determined pH–log k_0 profiles for the hydrolysis of β-aminocinnamonitrile (**2a**). Points are experimental and the curve is calculated from rate expression 4 and the derived rate constants of Table II.

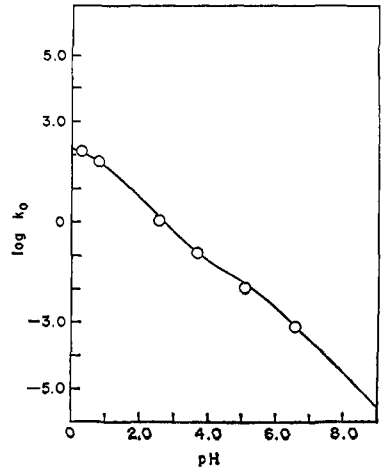

Figure 2. Spectrophotometrically determined pH–log k_0 profiles for the hydrolysis of β-amino-*p*-(N,N-dimethylamino)cinnamonitrile (**2c**). Points are experimental and the curve is calculated from rate expression 6 and the derived rate constants of Table II.

Underwood Programma 101 computer, using programs written by Dr. Donald Tanner, formerly of this laboratory.

Apparatus. Ultraviolet and visible spectra were measured on a Perkin-Elmer 350 recording spectrophotometer, which was also used for all initial kinetic runs. Infrared spectra were recorded by use of a Perkin-Elmer 137 sodium chloride spectrophotometer. All kinetic measurements were carried out on a Gilford 2000 spectrophotometer, a Zeiss M4Q III monochromator equipped with a Gilford multiple-sample absorbance recorder, a Zeiss PMQ II spectrophotometer, or a 13001 Durrum-Gibson stopped-flow spectrophotometer equipped with a Kel-F cell and valve block. The temperature in the spectrophotometer cell compartments was maintained at 30 ± 0.1° with water from large circulating baths. A Radiometer 22 pH meter equipped with a PHA 630 PA scale expander and Type GK 2021C combined electrode was used to determine pH. The electrode was stored at the temperature of the kinetic measurement.

Results

The pH–log rate profiles for the lyate hydrolysis of all enamines possessing nonionizable substituents have the general form of eq 2 as shown in Figure 1 for **2a**. The

$$k_{obsd} = k_r' \frac{a_H}{K_a + a_H} \tag{2}$$

linear portion of the curve with slope of −1 is attributed to catalysis by hydronium ion, and the plateau region is associated with a protonated form of the enamine. A scheme which involves a nonreactive N-protonated enamine together with an acid-catalyzed rate step is shown in (3). The rate of disappearance of enamine E is given

$$\begin{aligned} E + H^+ &\overset{K_a}{\rightleftharpoons} EH \\ E + H^+ &\xrightarrow{k_r} \text{products} \end{aligned} \tag{3}$$

by (4), which on combination with the empirical equation

$$k_{obsd} = k_r a_H \frac{K_a}{K_a + a_H} \tag{4}$$

(eq 2) leads to the plateau rate $k_r' = k_r K_a$. The points of Figure 1 are experimental and the curve theoretical having been derived from eq 4.

Enamines possessing ionizable substituents (**1c**, **2c**, **2d**) are characterized by plots exhibiting a deviation from linear slope of −1 in the area of the pK_a of the substituent group. An example of this type of plot is shown for **2c** in Figure 2. Presumably this change from linearity results from effectively changing the electronic nature of the substituent on protonation. A scheme such as shown in eq 5, including a rate step for the enamine with both protonated and nonprotonated substituents, leads to a more complex rate expression 6. The line of Figure 2 is theoretical and derived from eq 6. Evaluation of eq 4 and 6 to give the best fit of the

$$\begin{aligned} E + H^+ &\overset{K_1}{\rightleftharpoons} EH \\ E + H^+ &\xrightarrow{k_{r_1}} \text{product} \\ EH + H^+ &\overset{K_a}{\rightleftharpoons} EH_2 \\ EH + H^+ &\xrightarrow{k_{r_2}} \text{product} \end{aligned} \tag{5}$$

$$k_{obsd} = \left(\frac{k_{r_1}K_1 + k_{r_2}a_H}{K_1K_a + K_a a_H + a_H^2}\right) K_a a_H \tag{6}$$

experimentally obtained log k_{obsd}–pH profiles leads to values for the constants given in Table II.

Table II. Kinetic Constants for the Hydrolysis of Substituted Enamines

	X	σ[a]	Series I $k_r \times 10^4$ min^{-1}[b]	pK_{app}[c]	Series 2 $k_r \times 10^3$ min^{-1}	pK_{app}
a	H	0	1.41	0	1.31	1.10
b	CH_3	−0.17	2.24	0.5	1.90	1.25
c	$N(CH_3)_2$	−0.83	4.47	5.0	3.16	5.0
	$N^+H(CH_3)_2$	+0.82[d]	0.447	−2.30	0.562	0.5
d	COOH	+0.45			0.708	0
	COO^-	0.00			1.35	3.5
e	Cl	+0.23	1.26	−0.65	1.12	1.0
f	OCH_3	−0.27	2.51	0.75	2.09	1.50

[a] σ values from C. D. Ritchie and W. F. Sager, *Progr. Phys. Org. Chem.*, **2**, 323 (1964). [b] k_r refers to k_r of eq 4 for enamines containing nonionizable substituents. For enamines containing ionizable substituents, k_r refers to k_{r_1} and k_{r_2} of eq 6, for the nonprotonated and protonated substituent, respectively. [c] pK_{app} refers to pK_a of eq 4 for enamines containing nonionizable substituents. For enamines containing ionizable substituents, pK_{app} refers to pK_1 and pK_a of eq 6 for the singly and doubly protonated enamine, respectively. [d] σ for $N^+(CH_3)_3$.

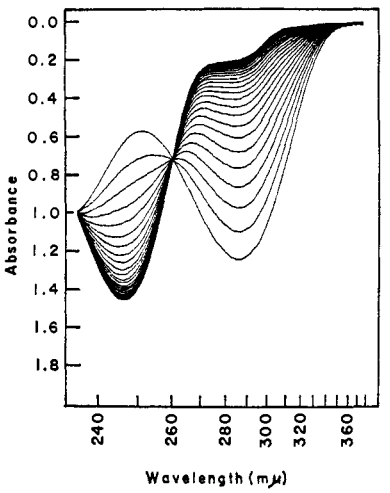

Figure 3. Spectral time study at pH 5.10 for the hydrolysis of β-aminocinnamonitrile (**2a**) in 1.0 *M* acetate buffer. Time interval is 6.5 min.

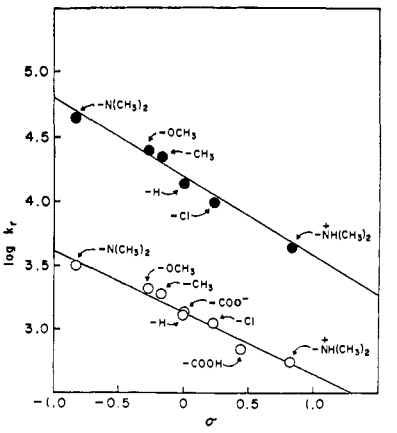

Figure 4. Hammett plot for the specific-acid catalyzed hydrolyses (k_r) of N-substituted (series **1**, closed circles) and C-substituted (series **2**, open circles) enamines. Values of all constants employed are provided in Table II.

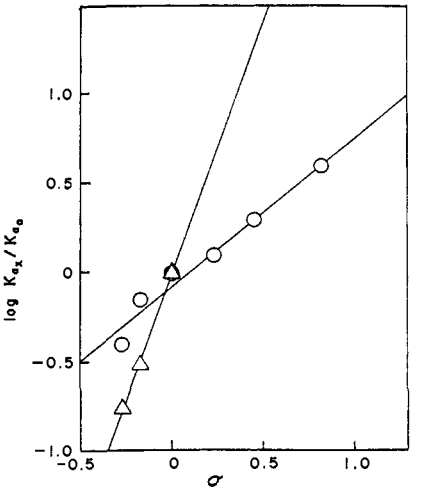

Figure 5. Hammett plot for the preequilibrium N-protonation (K_a) of N-substituted (series **1**, open circles) and C-substituted (series **2**, triangles) enamines. Values of all constants employed are provided in Table II.

Preliminary kinetic studies were carried out by repetitive scans of the reaction solutions of each enamine for at least one pH value. In all cases, tight isosbestic points were observed, as the enamine absorption decreased in intensity while the product absorption increased. A typical repetitive scan spectrum for **2a** is shown in Figure 3. In selected cases, runs were made at identical pH's following both disappearance of enamine and appearance of product, at the appropriate wavelength. Within experimental error, the rate of enamine disappearance was identical with the rate of ketone appearance. This fact, together with the observed isosbestic points in the repetitive scans, indicates that no intermediate accumulates during the hydrolysis of enamines of type **1** and **2**.

Comparison of k_r and K_a with σ for the substituent group shows a linear Hammett-type free energy relationship[24] (*i.e.*, log $k_r = \rho_k\sigma + C$, or log $K_{a_x}/K_{a_0} = \rho_{K_a}\sigma$). The plots shown in Figures 4 and 5 lead to an evaluation of $\rho_k = -0.612 \pm 0.006$ and $\rho_{K_a} = +2.80$ for **1**, $\rho_k = -0.489 \pm 0.005$ and $\rho_{K_a} = +0.84$ for **2**. Only when a clear break toward a plateau rate is observed in the pH–log rate profile (Figure 1) can pK_{app} be determined accurately. In the case of **1** this was possible when X = OCH_3 (**1f**), CH_3 (**1b**), and H (**1a**). Using ρ evaluated from these three pK_{app}, it was possible to estimate pK_{app} for **1** when X = Cl (**1e**) and X = $N^+H(CH_3)_2$ (**1c**) (Table II), both of which are less than zero, and outside the pH range of this investigation. In contrast, pH–log rate profiles for **2** exhibited discernible breaks in the line with slope of −1, and thus pK_{app} could be determined readily. Only in the case of **2d** (X = COOH) was no break observed at low pH, and this anomaly can be explained (see Discussion).

The hydrolysis of all enamines studied in the pH range 3–7 was catalyzed by buffer; at constant pH a linear relationship was obtained between k_{obsd} and [B_T]. This is described by eq 7 where k_0 is the lyate hydrolytic rate

$$k_{obsd} = k_0 + k_b[B_T] \quad (7)$$

constant at the pH employed (Figure 1 and 2) and k_b is the buffer catalytic rate constant. Rearrangement of eq 7 to eq 8 affords a means of separating general-

$$k_{obsd} - k_0 = k_{BH}[BH] + k_B[B] = \left(k_{BH} + k_B\frac{K_a}{a_H}\right)[BH] \quad (8)$$

acid (k_{BH}) and general-base (k_B) catalytic rate constants. Plots of ($k_{obsd} - k_0$)/[BH] *vs.* $1/a_H$ gave rise to lines of zero slope (*i.e.*, $k_B = 0$). Therefore, eq 8 can be reduced to eq 9. Combination of eq 7 and 9 results in

$$k_{obsd} - k_0 = k_b[B_T] = k_{BH}\frac{a_H}{K_a + a_H}[B_T] \quad (9)$$

eq 10, and k_{BH} is readily obtained at any given pH from

$$k_{BH} = k_b\frac{K_a + a_H}{a_H} \quad (10)$$

the slope of the line, k_b, obtained on serial buffer dilutions. The buffers employed and the pH range studied together with the catalytic rate constants are listed in Table III. A typical Brønsted plot derived from these data is shown in Figure 6, yielding $\beta = -0.67$ for the

(24) L. P. Hammett, "Physical Organic Chemistry," McGraw-Hill Book Co., Inc., New York, N. Y., 1940, Chapter 7.

Table III. General-Acid Rate Constants for Hydrolysis of Enamines[a]

Compound	H_3O^+ [b]	HCOOH[c]	CH_3COOH[d]	$H_2PO_4^-$ [e]	β[f]
1a	1.41×10^4	1.56 (2, 12)	4.35×10^{-1} (2, 12)	3.18×10^{-2} (2, 12)	−0.67
1b	2.24×10^4		4.60×10^{-1} (1, 3)	4.54×10^{-2} (3, 12)	−0.68
1e	1.26×10^4		1.30×10^{-1} (1, 3)	2.44×10^{-2} (1, 3)	−0.69
1f	2.51×10^4		1.12 (1, 3)	6.68×10^{-2} (1, 3)	−0.66
2a[g]	1.31×10^3	1.40×10^{-1} (1, 3)	3.87×10^{-3} (4, 11)	4.46×10^{-3} (2, 6)	−0.66
2b	1.90×10^3		5.65×10^{-3} (2, 6)	7.22×10^{-3} (1, 3)	−0.65
2e	1.12×10^3		1.89×10^{-3} (1, 3)	3.06×10^{-3} (1, 3)	−0.67
2f	2.09×10^3		3.78×10^{-3} (1, 3)	9.96×10^{-3} (1, 3)	−0.63

[a] All serial dilutions were run over a range of 0.1–1.0 M with $\mu = 1.0$. All rate constants in units of M^{-1} min^{-1}. Numbers in parentheses are the number of pH's, together with the number of k_{obsd} used to evaluate k_{BH}. For pH range of buffers employed, see Experimental Section. [b] $pK_a = -1.74$, assuming 55.5 M for activity of water in dilute, aqueous solution. [c] $pK_a = 3.77$ (G. Kortum, W. Vogel, and K. Andrussow, "Dissociation Constants of Organic Acids in Aqueous Solution," Butterworth and Co., Ltd., London, 1961. [d] $pK_a = 4.61$ [T. C. Bruice and B. Holmquist, *J. Amer. Chem. Soc.*, **89**, 4028 (1967)]. [e] $pK_a = 6.81$ (ref 29, p 134). [f] By method of least squares. [g] For reaction with H_3PO_4–KH_2PO_4 buffer at two pH's and six k_{obsd}, $k_{BH} = 8.37$ M^{-1} min^{-1}. K_a for $H_3PO_4 = 7.16 \times 10^{-3}$ [P. Saloma, L. L. Schaleger, and F. A. Long, *J. Amer. Chem. Soc.*, **86**, 1 (1964)]. For reaction with chloroacetate buffer at pH > pK_a where buffer catalysis was observed (one pH, three k_{obsd}), $k_{BH} = 8.07 \times 10^{-1}$ M^{-1} min^{-1}. pK_a for $ClCH_2COOH = 2.87$ (see reference in footnote *c*).

line which includes the point for hydronium ion (k_r).

At pH's lower than 4, depression of the rate of hydrolysis was observed with increasing concentration of added carboxylic acid buffer and/or organic solvent. This type of nonspecific buffer inhibition has been observed previously.[25] Inhibition by carboxylic acid

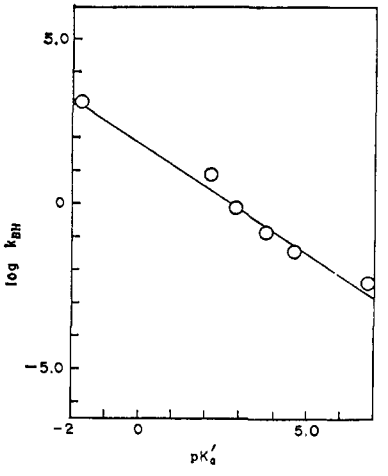

Figure 6. Brønsted plot of general acid catalyzed hydrolysis (k_{BH}) of β-aminocinnamonitrile (**2a**). Values of all constants employed are provided in Table III.

buffers was observed at pH values of *ca.* one unit below pK_a. As the pH was raised, a transition from buffer inhibition to buffer catalysis was observed. In contrast, H_3PO_4–KH_2PO_4 buffer, which presumably has little effect on the dielectric constant of the reaction solution, exhibited only general-acid catalysis in the same pH range.

In order to ascertain whether or not this inhibition could be attributed to a nonspecific solvent effect, various concentrations of organic solvents were added to the reaction mixture at several pH's. The observed rate data (Table IV) indicate that added organic solvents depress the rate in the pH range of 1–4. The intercept values (k_0) for plots of k_{obsd} *vs.* solvent or buffer concentration are identical, within experimental error, with a larger inhibition observed for solvent compared with the same concentration of buffer at any given pH above 1. At pH below 1, little or no solvent inhibition was observed although the data at the lower pH's are somewhat less reliable owing to an apparent initial reaction or complexation of some sort which leads to nonzero intercepts in the first-order rate plots.

That these solvent effects were not due entirely to hydronium ion induced changes in the activity of water was indicated by the fact that lithium chloride had no effect on the rate of hydrolysis at pH 4.08 at a concentration corresponding to hydronium ion at pH 1.84. In fact, lithium chloride had no effect on the rate of hydrolysis at pH 4.08 at concentrations ranging from 0 to 0.5 M. In contrast, hydrochloric acid added to 1.0 M acetic acid to bring the pH from *ca.* 4 to 1.84 resulted in a solution which inhibited the hydrolysis considerably compared to a solution at the same pH containing no acetic acid. It is known that the activity of water is similarly dependent on the concentration of lithium or hydronium ion.[26]

Substitution elsewhere on the molecule **1** was investigated, since σ–ρ treatment of the type shown in Figures 4 and 5 indicate only weak substituent effects in the series **1a–1f** and **2a–2f**. The k_r for ethyl β-anilinocrotonate (**1g**) is *ca.* 6×10^5 min^{-1} based on three sets of serial buffer dilutions run below pH 8. Above this pH, ester hydrolysis or some other base-catalyzed process leads to a plateau in the pH–log rate profile and a more complex reaction as indicated by spectral time studies. A two-point Hammett plot of log k_r *vs.* $\Sigma\sigma_I$[27] using k_r determined for **1a** and **1g** leads to a value of $\rho_I = -6.25$. However, **1h** (Y = CO_2Et, A = CN) hydrolyzes only very slowly at 30° in 1 N hydrochloric acid, and **1i** (Y = Z = CN) does not hydrolyze under identical conditions. It would appear that the true value of ρ_I for this system is more negative than −6.25. Hydrolysis of **4** in 28.5% aqueous ethanol at several pH's leads to $k_r = 41.7$ min^{-1}. This value must be corrected for rate differences arising from the change in solvent from water to 28.5% aqueous ethanol. The ratio, $k_{H_2O}/k_{28.5\%EtOH}$, determined for **1a** is 3.86, which when multiplied by k_r determined in 28.5% aqueous ethanol leads to k_{rH_2O} of *ca.* 1.6×10^2 min^{-1}. A value of $\rho_I = -12.8$ is obtained from a two-point Hammett plot of log k_r *vs.* $\Sigma\sigma_I$[27] for **1a** and **4**.

(25) (a) L. R. Fedor and T. C. Bruice, *J. Amer. Chem. Soc.*, 87, 4138 (1965); (b) E. G. Sander and W. P. Jencks, *ibid.*, 90, 4377 (1968).

(26) R. A. Robinson and R. H. Stokes, "Electrolyte Solutions," Butterworth and Co. Ltd., London, 1959, p 483.

(27) M. Charton, *J. Org. Chem.*, **29**, 1222 (1964).

Table IV. Effect of Added Solvents and Buffers on Hydrolytic Rates (μ = 1.0 *M* with KCl, T = 30°)

pH	a_H	Added solvent	k	% inhibition[a]
0.3	5×10^{-1}	*b*	65	
		1.0 *M* HOAc[b]	60–65	*Ca.* 0–10
1.3	5×10^{-2}	*b*	50	
		1.0 *M* HOAc[b]	38	24
1.84	1.445×10^{-2}	*b*	17.7[c]	
		0.1 *M* HOAc[b]	16.44	
		0.1 *M* HOAc[b]	16.87	
		0.5 *M* HOAc[b]	14.60	
		1.0 *M* HOAc[b]	9.14	48
		b	15.75[c]	
		0.0915 *M* EtOAc[b]	14.98	
		0.274 *M* EtOAc	13.33	
		0.457 *M* EtOAc[b]	10.74	
		0.091 *M* HOAcCl[d]	16.82	
		0.457 *M* HOAcCl[d]	14.83	
		0.914 *M* HOAcCl[d]	11.88	34
		0.914 *M* HOAcCl[d] + 1.0 *M* dioxane	6.71	57
		0.067 *M* H_3PO_4[e]	16.73	
		0.336 *M* H_3PO_4[e]	17.84	
		0.672 *M* H_3PO_4[e]	21.82	
3.25	5.623×10^{-4}	*f*	7.67×10^{-1}[c]	
		0.077 *M* HOFm[f]	7.67×10^{-1}	
		0.384 *M* HOFm[f]	7.66×10^{-1}	
		0.768 *M* HOFm[f]	7.65×10^{-1}	0
		0.1 *M* EtOAc[b]	6.20×10^{-1}	
		0.5 *M* EtOAc[b]	5.94×10^{-1}	
		0.768 *M* HOFm[f] + 1.0 *M* dioxane	5.75×10^{-1}	26
4.06	8.71×10^{-5}	*g*	12.5×10^{-2}[c]	
		0.078 *M* HOAc[g]	12.5	
		0.390 *M* HOAc[g]	13.0	
		0.781 *M* HOAc[g]	13.0	0
		0.274 *M* EtOAc[b]	11.1	
		0.457 *M* EtOAc[b]	10.7	
		0.781 *M* HOAc[g] + 1.0 *M* dioxane	8.55	30

[a] Per cent inhibition defined as per cent inhibition observed for linear decrease in k_{obsd} with increasing amounts of added solvent or buffer over the range 0–1 *M*. [b] HCl added to give desired a_H as measured by a glass electrode. [c] k_0 value obtained by extrapolation to zero buffer or solvent on plot of k_{obsd} *vs.* buffer or solvent concentration. [d] pH maintained with chloroacetic acid (HOAcCl) buffer. [e] pH maintained with phosphoric acid buffer. [f] pH maintained with formic acid (HOFm) buffer. [g] pH maintained with acetic acid (HOAc) buffer.

The relation between the position and its substituent effect on the rate of hydrolysis is summarized in (11).

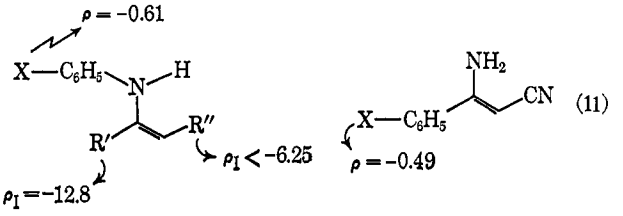

(11)

Discussion

The hydrolysis of all enamines investigated obeys either eq 4 or 6 with rate constants as given in Table II. Log rate–pH profiles (Figure 1) possess linear portions of slope −1, with a break at low pH leading to an observable plateau rate in cases where $pK_{app} > 1.0$. Comparison of ρ_k for hydrolysis of **1** and **2** reveals that electron withdrawal has a detrimental effect in both series. Inspection of Stuart–Briegleb molecular models reveals that maximum overlap of the lone pair of electrons on the enamine nitrogen with *both* the π electrons of the enamine carbon–carbon double bond *and* the π electrons of the substituted aniline of **1** occurs at the expense of increased steric strain imposed by several nonbonded interactions. In order for hydrolysis to occur, the lone pair of electrons on the enamine nitrogen must be in a position to overlap with the π electrons of the enamine carbon–carbon double bond. Steric restrictions then demand that the phenyl group be oriented in a position with the π electrons in a plane between 60 and 75° from the plane described by the nitrogen lone pair. Thus, resonance effects, as measured by σ_{para}, would not exert a large influence on the rate of hydrolysis, k_r. However, other conformations are possible which allow for maximum orbital overlap between the nitrogen lone pair and the π electrons of the aniline ring. These conformations are "nonproductive" conformations in that they do not lie on the hydrolysis reaction path, but could be involved in preequilibrium N protonations of eq 3 and 5. These considerations are borne out by the small substituent effect ($\rho = -0.61$) on k_r of **1**, compared with the large substituent effect ($\rho = +2.80$) on K_a of **1**. This is in sharp contrast with the large substituent effect ($\rho = -2.2$) observed in the acid-catalyzed hydrolysis of substituted phenyl vinyl ethers.[28] In these molecules the π electrons of the phenyl group, the oxygen lone pair, and the π electrons of the vinyl group all are colinear, leading to maximum orbital overlap and a large substituent effect. A similar argument can be put forth on the basis of inspection of molecular models of **2**. In this case, nonbonded interactions restrict the

(28) T. Fueno, I. Matsumura, T. Okuyama, and J. Furukawa, *Bull. Chem. Soc. Jap.*, 41, 818 (1968).

possibilities for maximum orbital overlap between the π electrons of the substituted phenyl group and the π electrons of the enamine carbon–carbon double bond, as long as the nitrogen lone pair is in the position of maximum orbital overlap with the π electrons of the carbon–carbon double bond required for hydrolysis. Again, it would appear that the π electrons on the phenyl group lie in a plane at least 60° away from the plane of the π electrons of the enamine double bond.

The small substituent effect ($\rho = -0.49$) on k_r of **2** is to be expected if resonance effects (σ_{para}) are not important in stabilization of the transition state. On the other hand, even though it is possible for other conformations to be involved in the preequilibrium protonation steps (eq 3 and 5), only inductive effects can influence K_a in **2**, leading to a low sensitivity of K_a to electron withdrawal on the phenyl ring ($\rho = +0.84$).

The very marked increase in substituent effects on enamine hydrolysis when the substituents are placed directly on the enamine double bond indicate that electronic reorganization is most critical at this bond. Comparison of the rate of hydrolysis (k_r) of β-anilinocrotononitrile (**1a**) with that for β-anilinocinnamonitrile (**4**) leads to an apparent ρ *ca.* −12.8. This great difference in rates may result from a combination of steric and electronic effects, although inspection of molecular models indicates no large difference between **1a** and **4** in the ability of the nitrogen lone pair and the enamine double bond to attain colinearity. Other reactions involving electrophilic substitution are associated with very large negative values of ρ; *e.g.*, bromination of monosubstituted benzenes by bromine in acetic acid, $\rho = -12.14$.[29] Another indication of the sensitivity of the enamine double bond to changes in electron density is shown by the differences in k_r in the series **1a**, **1g**, **1h**, and **1i**. The value of ρ is obviously much more negative than −6.25 obtained on comparison of k_r for **1a** and **1g**, since **1h** has k_r of *ca.* 10^{-3} min^{-1} and **1i** does not hydrolyze under the conditions employed in this investigation. It would be anticipated that electron-withdrawing substituents placed directly on the enamine double bond would enhance the stability of the enamine ground state and thus decrease the rate of hydrolysis. However, this cannot be the major factor in the observed electronic sensitivity in the hydrolytic reaction, since the keto–enol equilibria described by eq 12 obeys the Hammett equation[24] with $\rho = +0.788$.[30] Ground-

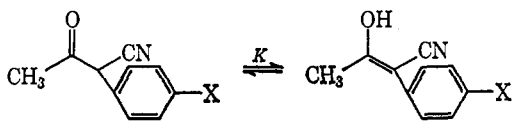

(12)

state stabilization, of course, is important in the ketimine–enamine equilibrium as with the keto–enol equilibrium. This can be inferred by the fact that more strongly electron-donating substituents, such as phenyl, destabilize the enamine ground state sufficiently that **3** exists exclusively in the imino form, which is rapidly hydrolyzed. The carbethoxy substituent of **1g** stabilizes the enamine form as indicated by the spectral characteristics. However, the rapid rate of hydrolysis of **1g** indicates that this stabilization is not as great as with the cyano substituents (**1a**). It is apparent that substituents on the β-carbon affect stability of the enamine ground state. The substituent effects at the various positions of the enamine molecule support (13) as a possible mechanism for the acid-catalyzed protonation step

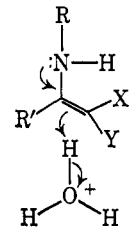

(13)

in enamine hydrolysis.

The value of ρ_{K_a} derived for **1** (+2.80) is in good agreement with that obtained for simple substituted anilines (+2.77).[31] All pK_{app}'s determined for **2** fit a Hammett plot[24] with $\rho_{K_a} = +0.84$, except **2d** (X = –COOH). In order to fit the ρ_{K_a} values for series **2**, the pK_{app} for **2d** would have to be *ca.* 0.80. Since no break at low pH is observed in the pH–log rate profile for **2d**, $pK_{app} \leq$ zero. It is known that amino acids exist as dipolar ions, even when the amino and carboxyl groups are well separated.[32] In the case of **2d**, an additional equilibrium, K_Z, becomes important, leading to a low pK_{app} and a significant positive deviation in the Hammett plot. This can be represented as in eq 14 which leads to expression 15. If the enamine does not exist to

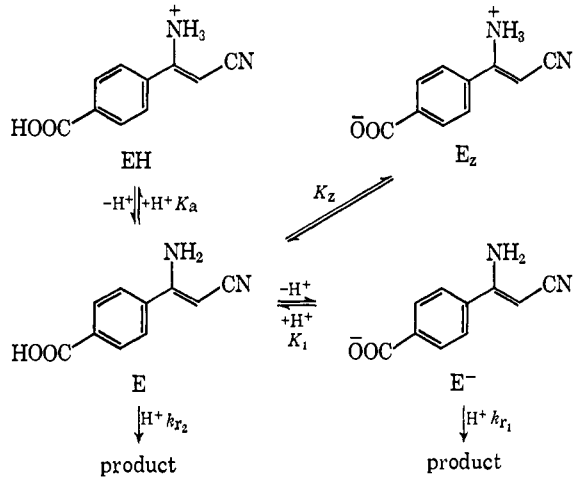

(14)

$$k_{obsd} = \left(\frac{(k_{r_1}K_1 + k_{r_2}a_H)}{K_1K_a + K_aa_H(1 + K_Z) + a_H^2}\right)K_aa_H \quad (15)$$

any appreciable extent as the dipolar ion, E_Z, then $K_Z \ll 1$, and eq 15 reduces to eq 6. If, however, the enamine is primarily in the form of the dipolar ion, then $K_Z \gg 1$, and eq 16 is the resultant expression. At high a_H, K_1

$$k_{obsd} = \left(\frac{k_{r_1}K_1 + k_{r_2}a_H}{(K_1 + K_Za_H)K_a + a_H^2}\right)K_aa_H \quad (16)$$

$\ll K_Za_H$, and K_{app}, usually associated with the plateau rate at high a_H, will not be simply K_a, but rather K_ZK_a. As mentioned above, in the case of **2d**, $pK_{app} \leqq$ zero, and ρ_{K_a} for **2** requires $pK_a = 0.80$ for this enamine.

(29) H. C. Brown and Y. Okamoto, *J. Amer. Chem. Soc.*, 80, 4979 (1958).
(30) M. J. Malawski and W. Czerka, *Ann. Chem.*, 34, 107 (1960); *Chem. Abstr.*, 54, 23632*f* (1960).
(31) H. H. Jaffé, *Chem. Rev.*, 53, 191 (1953).
(32) E. J. Cohn and J. T. Edsall, "Proteins, Amino Acids and Peptides," Reinhold Publishing Corp., New York, N. Y., 1943, p 96.

Therefore, since $K_{app} = K_Z K_a \leqq 1.0$, $K_Z \geqq 6.33$, or at least 85% of enamine **2d** exists in the dipolar form, E_Z. This is in accord with literature values[32] of K_Z for simple amino acids such as *m*-aminobenzoic acid ($K_Z = 2.3$).

The buffer catalysis observed in this investigation is made more complex by the presence of a strong inhibitory nonspecific solvent effect. The increased amount of inhibition induced by organic solvent *vs.* organic acid buffers at a given pH indicates that buffer effects by organic buffers are a combination of inhibition arising from a change in the solvent polarity and general-acid catalysis by the buffer. The Brønsted plot (Figure 6) shows that a line drawn through the points for H_3O^+, H_3PO_4, and $H_2PO_4^-$ lies somewhat above the points for the organic carboxylic acids. Any mechanistic conclusions drawn from Brønsted plots using organic acids as the general-acid catalyst may be of questionable validity since the "general-acid rate constant" derived from eq 10 could be a combination of general acid catalysis and acid inhibition, the latter arising from the change in solvent polarity with increasing amounts of the free acid form of the buffer. The Brønsted plots should be viewed in this light, although the values for β of -0.63 to -0.69 (Table III) are in good agreement with β of -0.66 obtained for the general acid catalyzed hydrolysis of ethyl vinyl ether.[33] If carboxylic acids of low dielectric constant are used to maintain constant pH (*e.g.*, chloroacetate, acetate, etc.), the effect of solvent on rate should be investigated and, if necessary, only inorganic acids used as buffers. The fact that β derived from k_{BH} for H_3O^+, H_3PO_4, and $H_2PO_4^-$ for **2a** (Figure 6) is *ca.* 0.65, and thus very close to all β values derived from all general acids (Table III), indicates that the data in Table III are of use in elucidating the nature of proton transfer.

Comparison of the ρ values summarized in (11) and β determined for **1** and **2** reveals an apparent conflict in the data. The inference, based on the value of β of *ca.* 0.65, is that the proton is slightly more than halfway transferred from the general acid to the enamine in the transition state. This would suggest (17) as the mech-

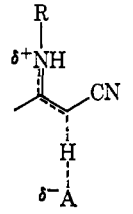

(17)

A = H_2O, $H_2PO_4^-$, $ClCH_2COO^-$, $HCOO^-$, CH_3COO^-, HPO_4^{2-}

anism for the general acid catalyzed protonation step in enamine hydrolysis. However, this mechanism would also predict a considerable buildup of positive charge on the enamine nitrogen. It is possible that the fact that

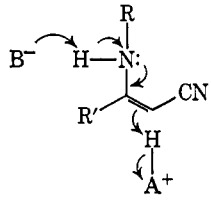

(18)

A = H_2O

there is only minimal orbital overlap between the lone pair of the nitrogen and the π electrons of the phenyl ring, as discussed earlier, would lead to a ρ_k of less than one-half that of ρ_{K_a} (-0.61 *vs.* $+2.80$).

A kinetically equivalent mechanism involving general-base, specific-acid catalysis such as depicted in (18) also resolves the apparent conflict. This type of buffer catalysis can be described by eq 19 which, when

$$k_{obsd} - k_0 = k_{BH}' a_H \left(\frac{K_a}{K_a + a_H}\right)[B_T] \qquad (19)$$

equated with eq 10 for the kinetically equivalent general-acid catalysis, leads to eq 20. The general-acid

$$k_{BH}' = \frac{k_{BH}}{K_a} \qquad (20)$$

rate constants (k_{BH}) listed in Table III can be converted to the general-base, specific-acid rate constants (k_{BH}') by use of this relationship, and a Brønsted plot of k_{BH}' *vs.* pK_a' for **2a** gives a value of $\alpha = +0.34$. Thus, proton transfer to the general base is not very far advanced in the transition state, and proton abstraction avoids a buildup of formal positive charge on nitrogen in the transition state and a low sensitivity to changes in substituents on the anilino moiety of **1**. However, inspection of the retrograde reaction indicates that the principle of microscopic reversibility would require a thermodynamically unfavorable dissociation of a proton from the protonated imine in a preequilibrium step, followed by readdition of a proton to the imino nitrogen *via* general-acid catalysis coupled with proton abstraction from the β-carbon in the rate step. This is not chemically reasonable. Proton abstraction by water would be required in the retrograde reaction and this is also unreasonable in view of the fact there would be stronger bases than water present in solution capable of effecting proton abstraction. As a result, (18) can be eliminated as a possibility for the mechanism of enamine hydrolysis and, therefore, (17) remains as the most reasonable mechanism.

The reaction scheme of eq 21 ($k_1/k_{-1} = K_2$) describes the systems under discussion. Equations 4 and 6 are

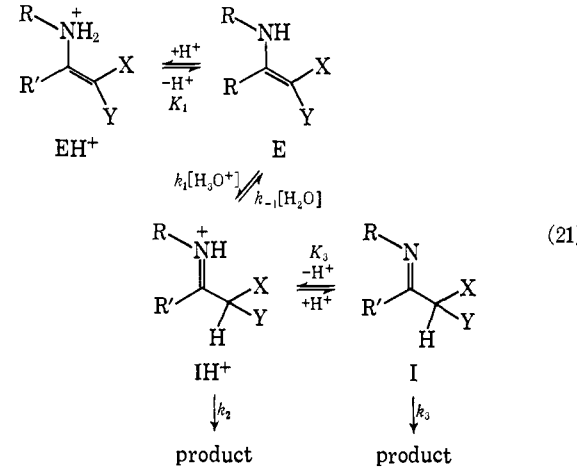

(21)

obtained if one assumes rate-determining tautomerism of E to IH^+, followed by a rapid hydrolysis of IH^+ to products; *i.e.*, $k_2 \gg k_1 a_H$. If, however, one assumes preequilibrium protonation of E to give either EH^+ or IH^+, eq 22 is obtained, which is of the general form of

(33) M. W. Kreevoy and R. Eliason, *J. Phys. Chem.*, 72, 1313 (1968).

$$k_{obsd} = \frac{k_2 a_H}{K_3 + K_2}\left[\frac{\frac{K_1K_3 + K_1K_2}{K_1 + K_2}}{\frac{K_1K_3 + K_1K_2}{K_1 + K_2} + a_H}\right] + \frac{k_3K_3}{K_3 + K_2}\left[\frac{\frac{K_1K_3 + K_1K_2}{K_1 + K_2}}{\frac{K_1K_3 + K_1K_2}{K_1 + K_2} + a_H}\right] \quad (22)$$

eq 23, where k_1', k_2', and K_{a_1} are as defined. Since k_2

$$k_{obsd} = k_2' a_H\left[\frac{K_{a_1}}{K_{a_1} + a_H}\right] + k_3'\left[\frac{K_{a_1}}{K_{a_1} + a_H}\right]$$

$$k_2' = \frac{k_2}{K_3 + K_2} \quad (23)$$

$$k_3' = \frac{k_3K_3}{K_3 + K_2}$$

$$K_{a_1} = \frac{K_1(K_2 + K_3)}{K_1 + K_2}$$

$\gg k_3$, and $K_3 < 1$, then $k_2 \gg k_3K_3$, and $k_2' \gg k_3'$. It follows that in the low pH region, $k_2'a_H \gg k_3'$ and thus the second term of eq 23 can be ignored at low pH. Equation 22, therefore, can be reduced to the form of eq 4, and thus the two situations, *i.e.*, k_1 or k_2 rate determining, lead to the same general form of the rate equations, eq 2 and 4. That k_1 is, in fact, rate determining over the major portion of the pH region investigated is indicated by the observed general-acid catalysis by buffers. General-acid catalysis would be expected for the tautomeric change

$$E \xrightarrow{k_1} IH^+ \quad (24)$$

However, with k_2 rate determining, one would not expect to observe general-acid catalysis in the spontaneous hydrolysis of IH^+. At low pH, k_1a_H could approach or even surpass k_2 in magnitude. Thus, a change in rate-determining step from k_1 to k_2 would be observed. Since these two situations have been shown to give rise to the same general form of rate expression, eq 4, it would ordinarily be difficult to detect this change in rate-determining step. However, the observed solvent effects on k_{obsd} at low pH are difficult to explain without invoking a change in rate-determining step as discussed above. A solvent-induced change in K_1 would result in a change in the ratio of $E:EH^+$. If this were so, the plateau rate associated with K_1 should be either increased or decreased as the solvent polarity changes. However, this is not observed. A rate depression is observed at pH 1.3–4 (Table IV), and as one proceeds to lower pH, instead of leading to a depressed or enhanced plateau rate, added organic solvents have no effect on k_{obsd}. This behavior can only be rationalized by transition from $k_2 \gg k_1a_H$ to $k_1a_H \gg k_2$ with increasing a_H. On decreasing the pH, k_2 becomes rate determining and IH^+ is formed in a preequilibrium. Over-all, then, increased concentration of nonpolar organic solvents would be expected to depress k_{obsd} at pH's where k_1 is rate determining, wheras when k_2 is rate determining and IH^+ is formed in a preequilibrium, no rate depression should be observed with increased concentration of organic solvents. This predicted behavior is in accord with the experimental facts, thus lending credence to the proposed mechanism.

In a study of tertiary enamines of type **5**, Stamhuis, *et al.*,[14] concluded that three different rate-determining

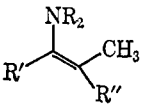

5, R_2N = morpholino, piperidino, and pyrollidino; R′ = H; R″ = CH_3

steps were involved, depending on the pH of the reaction (*cf.* Scheme V, ref 14b); *i.e.*, a transition from rate-determining protonation of the β-carbon, to general base catalyzed hydrolysis of the immonium ion, to hydrolysis of the carbinolamine, as the acidity is increased from pH 14 to $H_0 = -2$.

As this investigation was being completed, a report by Sollenberger and Martin[34] appeared in which the hydrolysis of enamines of type **5** was reinvestigated, where R′ = substituted phenyl, R″ = CH_3, and R_2N are as in ref 14, with the addition of R_2N = dimethylamino. Owing to the preliminary nature of the report, no direct comparison can be made with the work of Stamhuis and coworkers.[14] However, both groups of investigators come to similar conclusions concerning changes in the rate-determining step with pH, with the exception that Sollenberger and Martin[34] conclude that the rate decrease noted at lower pH results from changes in the activity of water and acid inhibition of carbinolamine zwitterion formation, rather than acid inhibition of carbinolamine cleavage as proposed by Stamhuis, *et al.*[14b] Clarification of ambiguities in the mechanism of hydrolysis of **5** presumably will be presented in a forthcoming publication by Sollenberger and Martin.

The major contribution of the present research is to delineate the influence of structural changes on the stability of enamines and their hydrolysis. Based on these observations it would appear that the enamines purported to be involved in enzymatic aldol condensations and decarboxylations (Scheme I) are not stabilized in the enamine form and most certainly would exist primarily as the imine tautomer. Since the tautomerization step (k_1) for all enamines investigated has been shown to exhibit general-acid catalysis, yielding eventually to the protonated imine, the principle of microscopic reversibility would predict that the reverse tautomeric change would involve general-base catalysis on the protonated imine. The imine formed between the ε-amino group of lysine and the carbonyl group of substrate presumably is protonated at physiological pH. This statement is based on the fact that pK_a values for imines are *ca.* two to four pH units below that of the parent amine,[35] thus giving a pK_a of *ca.* 8 for imines derived from lysine ($pK_a = 10.53$[36]). In the enzymatic reaction it would appear that formation of the thermodynamically less stable enamine is catalyzed by a general base on the enzyme, *i.e.*, (25). This is in accord with the conclusion reached

(34) (a) P. Y. Sollenberger and R. B. Martin, Abstracts, 156th National Meeting of the American Chemical Society, New York, N. Y., Sept 1968, Organic Abstract No. 66. (b) P. Y. Sollenberger, Ph.D. Thesis, University of Virginia, 1968.

(35) (a) E. J. Stamhuis, W. Maas, and H. Wynberg, *J. Org. Chem.*, 30, 2160 (1965); (b) E. H. Cordes and W. P. Jencks, *J. Amer. Chem. Soc.*, **85**, 2843 (1963).

(36) Reference 32, p 85.

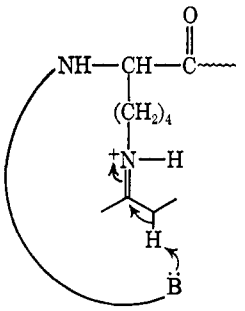

(25)

by Bender and Williams[9] based on their studies involving amine-catalyzed enolization of acetone.

It is interesting to note that there is no evidence from the present investigation to support a concerted acid–base catalysis in imine–enamine tautomerization such as that proposed for keto–enol tautomerization and investigated in the accompanying paper.[10] The absence of any base-catalyzed hydrolysis is exemplified by the fact that hydrolysis of the cyano group of **2a** to the corresponding amide, **6**, results in preference to hydrolysis of the enamine to yield the β-keto nitrile or β-keto amine.[37] Thus, whereas Banks reported concerted acid–base catalysis in the ketonization of oxaloacetic acid enol (26a)[38] there is no evidence to support such a mechanism in imine–enamine tautomerization (26b).

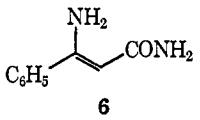

6

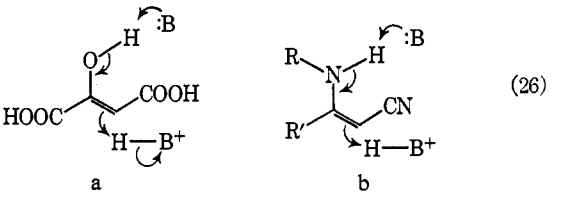

a b

(26)

Acknowledgment. This work was supported by Grant GB 5294X from the National Science Foundation and Grant AM 09171-05 from the National Institutes of Health.

(37) A. Dornow, I. Kühlcke, and F. Baxmann, *Chem. Ber.*, **82**, 254 (1949).
(38) B. E. Banks, *J. Chem. Soc.*, 63 (1962).

Intramolecular Amine-Catalyzed Ketone Enolization. A Search for Concerted Intramolecular General-Base, General-Acid Catalysis

James K. Coward[1] and Thomas C. Bruice[2]

Contribution from the Department of Chemistry, University of California at Santa Barbara, Santa Barbara, California 93106.
Received February 10, 1969

Abstract: A series of ketones possessing one or two tertiary amino groups has been prepared and their rate of enolization determined. Rates of enolization were determined by use of one or more of the following kinetic procedures: (a) zero-order kinetics employing ketone in excess of the iodine trapping reagents (spectrophotometric); (b) first-order kinetics employing iodine trapping reagents in great excess over ketone (pH-stat); and (c) first-order rates of racemization (polarimetric). Limitations to the application of these techniques are discussed. For those cases where more than one technique could be brought to bear on any one ketone the determined rate constants were in fair agreement. From pH–log k_{obsd} profiles for both mono- and diamines it is apparent that the mechanism of enolization is dependent upon the state of ionization of a single amino group (*i.e.*, for the diamino ketones there is no evidence for a concerted intramolecular general-acid and general-base catalyzed enolization).

A classic reaction subject to catalysis by general acids and general bases is the enolization of ketones. The possibility exists, therefore, for a concerted acid–base catalysis, indicated by the appearance of a termolecular, or product, term in the rate expression (*i.e.*, *k*[general base][general acid][ketone]). The presence or absence of this product term, and its possible significance, have been the subject of a prolonged controversy.[3] A major criticism of the termolecular mechanism has been that the magnitude of the product term is very small compared to the catalytic terms for either general-acid or general-base catalysis.[4] However, in one of the few kinetic studies involving the direct measurement of the rate of ketonization of an enol, Banks[5] reported a product term contribution of 15–23% in the case of triethanolamine or imidazole catalysis. Other workers have found smaller contributions of the product term,[6,7]

(1) Postdoctoral Fellow of the National Institutes of Health, 1966–1968.
(2) To whom inquiries should be addressed.
(3) For reviews, see (a) T. C. Bruice and S. J. Benkovic, "Bioorganic Mechanisms," Vol. I, W. A. Benjamin, Inc., New York, N. Y., 1966, p 334; (b) J. Hine, "Physical Organic Chemistry," 2nd ed, McGraw-Hill Book Co., Inc., New York, N. Y. 1962, p 109.
(4) K. J. Pedersen, *J. Phys. Chem.*, **38**, 590 (1934).
(5) B. E. Banks, *J. Chem. Soc.*, 63 (1962).
(6) R. P. Bell, "The Proton in Chemistry," Cornell University Press, Ithaca, N. Y., 1959, pp 124–154, and references therein.
(7) M. L. Bender and A. Williams, *J. Amer. Chem. Soc.*, **88**, 2502 (1966).